

You Only Need Two Detectors to Achieve Multi-Modal 3D Multi-Object Tracking

Xiyang Wang Jiawei He Chunyun Fu* Ting Meng Mingguang Huang

Chongqing University

{wangxiyang, hejiawei, fuchunyun}@cqu.edu.cn, {mengting, huangmingguang}@stu.cqu.edu.cn

Abstract: Firstly, a new multi-object tracking framework is proposed in this paper based on multi-modal fusion. By integrating object detection and multi-object tracking into the same model, this framework avoids the complex data association process in the classical TBD paradigm, and requires no additional training. Secondly, confidence of historical trajectory regression is explored, possible states of a trajectory in the current frame (weak object or strong object) are analyzed and a confidence fusion module is designed to guide non-maximum suppression of trajectory and detection for ordered association. Finally, extensive experiments are conducted on the KITTI and Waymo datasets. The results show that the proposed method can achieve robust tracking by using only two modal detectors and it is more accurate than many of the latest TBD paradigm-based multi-modal tracking methods. The source codes of the proposed method are available at <https://github.com/wangxiyang2022/YONTD-MOT>

Index Terms: 3D MOT, Camera and LiDAR fusion, object detection and tracking.

I. INTRODUCTION

Multi-object tracking is intended for determining the position and identity, i.e., trajectory ID, of objects in each frame of an image sequence or point cloud data. Depending on the scene, multi-object tracking can be divided into 2D tracking and 3D tracking. 2D tracking is commonly applied in fields such as monitoring and security based on image data, while 3D tracking is suitable for fields such as autonomous driving and robotics based on point cloud data. Currently, common multi-object tracking paradigms include tracking-by-detection [1-7], joint detection and embedding [8, 9], tracking-by-attention [10-12], and joint detection and tracking [13-15].

Multi-object tracking methods based on a single modal often underperform those based on multi-modal fusion due to lack of sufficient information about objects. Existing multi-object tracking methods based on multi-modal fusion are commonly based on the tracking-by-detection paradigm [16-19], where 3D detectors [20-22] and 2D detectors [23-25] are used to detect objects in point clouds and images, respectively. Feature fusion or post-fusion is then performed to realize fusion of 3D detection and 2D detection. Finally, a data association strategy is applied for matching. This paradigm has detection and data association respectively in two modules, and fails to effectively integrate them, thereby requiring a complex data association strategy to achieve correct matching between detections and trajectories. For this

reason, it cannot be used to achieve end-to-end multi-object tracking, as shown in Fig. 1.

Although there are some regression-based tracking frameworks [13, 14], which use two-stage 2D detectors, take historical trajectories as proposals for regression, and then perform association with detections in the current frame through non-maximum suppression, these methods are all 2D tracking based on images and cannot be used to achieve 3D tracking in autonomous driving scenarios. Additionally, single modal data makes it difficult to achieve robust tracking. There are some multi-modal fusion 3D tracking methods based on the JDE paradigm [26, 27], which fuse feature extraction into detectors, but in these methods complex data association processes are required. In order to explore correlation between detection and data association based on multi-modal data, and integrate detection and tracking in the same model, an innovative end-to-end multi-object tracking method named YONTD-MOT is introduced in this paper based on multi-modal fusion. Unlike previous multi-modal fusion methods, this method fuses data association into post-processing of the original two-stage detector, thereby eliminating the need for a complex data association module. For the purpose of the present work, we studied the confidence of historical trajectory regression to analyze the trajectory status, based on which a module incorporating trajectory regression confidence is proposed and used to guide Non-Maximum Suppression (NMS), so as to achieve ordered and robust association.

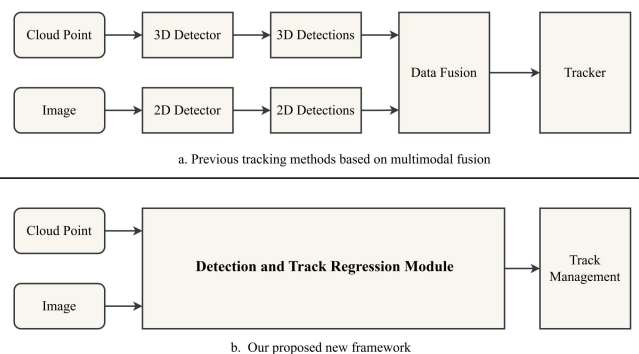


Fig. 1 (a) In prior work, 2D detection and 3D detection are fused before tracking. (b) In the present work, an end-to-end multi-object tracking framework is proposed based on multi-modal fusion.

Main contributions of this paper include:

- An end-to-end multi-modal fusion tracking method is

*Corresponding author

proposed, which requires no complex data association process in the classic TBD paradigm, and allows use of the same model to perform both detection and tracking without the need for additional detector training.

- The concept of historical trajectory confidence is introduced for investigating trajectory performance in different states, and classification is made accordingly. A confidence fusion module is further proposed to guide ordered matching of detections and trajectories.
- The method proposed in the present work can achieve excellent tracking performance on different datasets (KITTI and Waymo), with state-of-the-art performance among all multi-modal fusion methods on the KITTI dataset and the highest AssPr (91.74%) among all single-modal and multi-modal methods.

II. RELATED WORKS

A. MOT Based on Tracking-By-Detection

The TBD paradigm first proposed by SORT [1] has become a mainstream multi-object tracking framework. It mainly consists of two steps: object detection and data association. Object detection is used to detect the position information of objects in the current frame, while data association is used to achieve the optimal matching between historical trajectories and detections in the current frame. DeepSORT [2] has a pedestrian re-identification (Re-ID) network added to the framework of SORT, and this has greatly improved the tracking performance by learning the appearance features of objects and combining them with IoU to calculate the similarity. In [28], a multi-object tracking method suitable for high frame rate scenes is proposed, highly relying on two assumptions: sufficiently high frame rate of the tracking scene and sufficiently high accuracy of the detector to produce only one detection result for each object to be tracked in each frame. With these two assumptions satisfied, simply IoU is used as the similarity for matching. This method features fast tracking, but the tracking robustness is limited. Bytetrack [3] opined that low-confidence detection results should not be filtered out during tracking, and conducted a large number of experiments to prove that retaining low confidence detections could produce more TP (True Positive) than FP (False Positive). These methods have generally considered detection and data association in two independent modules, and ignored correlation between them.

B. MOT Based on Joint Detection and Embedding Learning

Although the tracking framework based on the TBD paradigm can achieve good performance, it requires an additional feature extraction network to obtain appearance information of objects, and this increases the computational complexity of the entire tracking process. Joint Detection and Embedding Learning (JDE) [8] integrates an object detection module and an appearance feature extraction module into one network, having greatly improved the processing speed of multi-object tracking algorithms. However, FairMOT [9] holds that the anchor-based detector used in the JDE algorithm is unsuitable for learning the ReID information of objects since an object may be detected by multiple anchors and this blurs appearance information. In addition, deviation of the

actual object center from the center of a detecting anchor may lead to great ambiguity during network training. Considering the foregoing, FairMOT proposed, based on JDE, use of an anchor-free object detection method to estimate the center and position of an object on a high-resolution feature map, and addition of parallel branches to obtain Re-ID features, having further improved the tracking performance. Though incorporation of some steps in data association into a detection module is attempted in this paradigm, a complex data association strategy is still required in subsequent steps.

C. MOT Based on Attention

The attention mechanism [29] was originally applied in the field of natural language processing. Due to its powerful performance, it was later introduced to the computer vision field, bringing about a series of Transformer-based object detection algorithms, such as DETR [30], Deformable DETR [31], and ViT-FRCNN [32]. Subsequently Transformer gradually found its application in the multi-object tracking field. TransTrack [10] uses a query-key mechanism to track objects of the current frame and detect new objects based on the trajectory features from the previous frame. In the query-key mechanism, the feature map of the current frame is taken as the key, while historical trajectory features and a set of learnable vectors are taken as the query. The learnable query is pre-trained to detect new objects. Historical trajectory features are generated by past frame detections to associate objects and output trajectory boxes for tracking. TrackFormer [11] takes each query as an object and performs spatio-temporal tracking of objects in a self-regressive manner. Namely, a new object appearing in a frame is detected by static object queries to generate a new trajectory and taken as a query for subsequent tracking. As a new Tracking-By-Attention paradigm, TrackFormer can realize simultaneous object detection and data association, and attain SOTA performance on the MOT17 [33] dataset. TransMOT [12] uses a spatio-temporal graph Transformer to build spatial relations between objects by considering trajectories as sparse weighted graphs, and introduces a cascaded matching framework to handle low-score detections and long-term occluded trajectories, having achieved state-of-the-art tracking performance on MOT17 [33] and MOT20 [34] datasets. Although Transformer-based methods can achieve high tracking performance, they are characterized by extremely high computation cost is huge, and most of them are based on 2D tracking of images.

D. MOT Based on Joint Detection and Tracking

In multi-object tracking based on the tracking-by-detection paradigm, detection and tracking are separate, and it is impossible to optimize the tracking performance by jointly training tracking and detection. Tracktor [13] uses a two-stage detector, in which bounding boxes tracked in the previous frame serve as proposals for the current frame detection. In this model, regression is performed to derive positions in the current frame and then non-maximum suppression is used to realize tracking and detect new objects in the current frame. In this way, detection and tracking are integrated in a single model. Based on Tracktor, FFT [14] has an optical flow prediction branch added to further improve the tracking performance. Nevertheless, these methods cannot deliver robust tracking performance due to single modal data, though

detection and tracking are integrated into a single module; moreover, these methods perform 2D tracking based on images, and are incapable of 3D tracking in the world coordinate system.

In this paper, a 3D MOT framework is proposed based on multi-modal fusion for joint detection and data association. The framework can effectively fuse different modal data and realize stable 3D tracking simply relying on the detection network. Besides, a historical trajectory regression confidence-guided NMS strategy for detection and trajectory is also proposed for the first time to improve the robustness of 3D MOT.

III. PROPOSED METHOD

The multi-modal fusion-based multi-object tracking method proposed in this paper is structured as shown in Fig. 2. The structure consists of three modules: data input module, detection and trajectory regression module, and track management.

The detection and trajectory regression module consists of several major components, including two-stage 2D and 3D detectors, confidence fusion, and NMS based on trajectory regression confidence. First, bounding boxes in the current frame are derived by a two-stage 3D detector through detection in the current frame point cloud, and then 3D trajectories state of the previous frame are predicted by a

Kalman filter. Motion transformation of the vehicle from the previous frame to the current frame is derived from GPS/IMU data, and then used for pose compensation to the predicted trajectory state. Next, the predicted trajectories after motion compensation are used as proposals, which, together with cloud information of the current frame point, is input into the two-stage detector for regression, so as to obtain the pose and confidence of the previous frame trajectories in the current frame. Meanwhile, the regressed 3D trajectories are projected onto a 2D image; the projected 2D trajectories and the current frame image are input into the image-based two-stage detector to obtain the confidence of the trajectories. Then, confidence of the regressed trajectories obtained from the 3D and 2D detectors are fused with the historical confidence. Finally, the fused trajectories confidence is used to guide NMS in trajectory and detection; namely, NMS in the current frame detections are performed in sequence according to the ranking of trajectories confidence level to achieve data association.

The trajectory management module is used to manage new, updated, dead and other states of a trajectory and to post-process the trajectory. For trajectory state management strategy, that proposed in our previous work, DeepFusionMOT [16], is adopted.

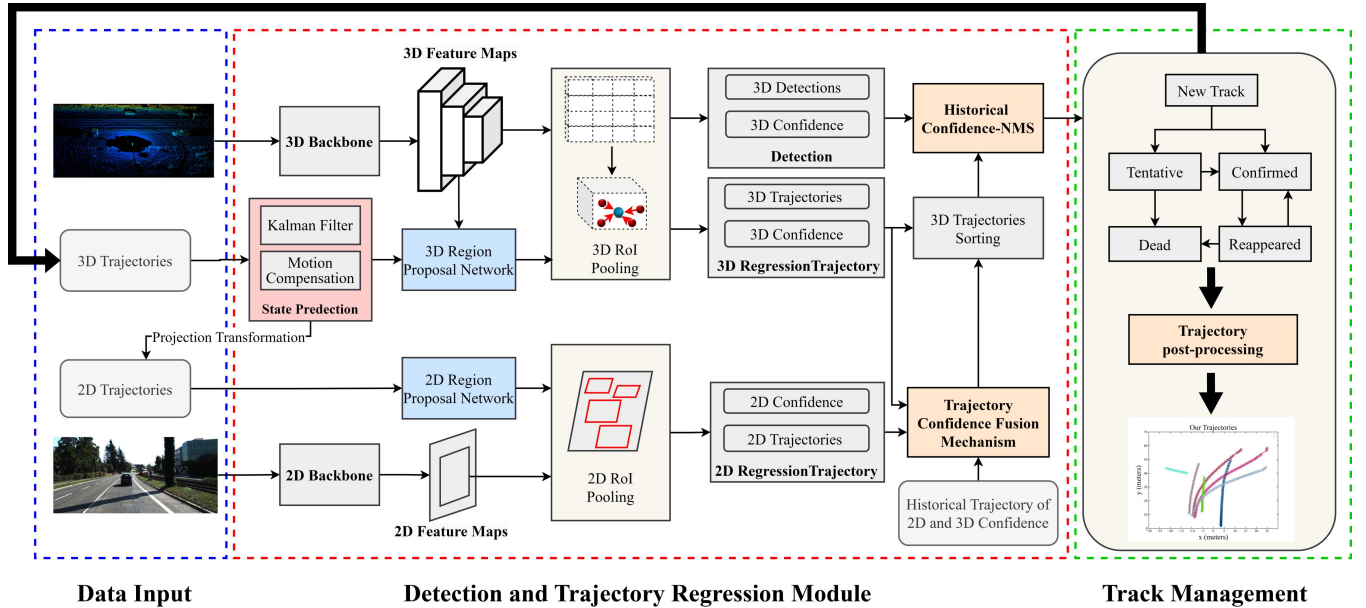


Fig. 2 An overview of the proposed YONTD-MOT framework.

A. Any Two stage 2D and 3D detector

The proposed method requires use of two-stage detectors, which includes a Region Proposal Network. For 2D detection, Faster R-CNN [25] is used and for 3D detection, CasA [35] is used (or alternatively, any other two-stage detector can be used). The detectors are trained on the KITTI and Waymo datasets.

Two-stage detectors first extract candidate regions of objects through the Region Proposal Network, and then classify and locate the extracted regions through a regression network. In the tracking process, a 3D detector is first used for detection in the point cloud of the current frame, and $D_t = \{D_t^1, D_t^2, \dots, D_t^n\}$ can be obtained. Then 3D trajectories, $T_{t-1}^{3D} = \{T_{t-1}^1, T_{t-1}^2, \dots, T_{t-1}^m\}$, in the previous frame are taken as Proposals, and preset Proposals are classified and located by using the 3D detector to obtain the regression trajectories of

the current frame, $T_t^{3D} = \{T_t^1, T_t^2, \dots, T_t^m\}$, and their 3D trajectory regression confidence, $S_t^{3D} = \{S_t^1, S_t^2, \dots, S_t^m\}$. At the meantime, the regressed 3D trajectories T_t^{3D} are projected onto an image to form 2D trajectories T_{t-1}^{2D} , which are taken as Proposals and input into the 2D detector for classification and regression to obtain the 2D trajectory regression confidence $S_t^{2D} = \{S_t^1, S_t^2, \dots, S_t^m\}$.

B. State Prediction

State prediction is realized through two modules, i.e. Kalman filtering and motion compensation modules. The trajectory state T_{t-1}^i , of the previous frame is first predicted by using a constant velocity model (Equation 1) to obtain the predicted state \hat{T}_t^i at discrete time t . The trajectory state can be represented by an 11-dimensional vector $T_{t-1}^i = [x_{t-1}^i, y_{t-1}^i, z_{t-1}^i, \theta, l, w, h, s, v_x^i, v_y^i, v_z^i]^T$, where $x_{t-1}^i, y_{t-1}^i, z_{t-1}^i$ represent coordinates of the i -th trajectory in the camera coordinate system, θ represents the heading angle, l, w, h represent the length, width and height of the i -th trajectory, s is the confidence score, and v_x^i, v_y^i, v_z^i represent the velocity along corresponding coordinate axes. The state prediction process can be expressed as follows:

$$\hat{T}_t^i = AT_{t-1}^i. \quad (1)$$

$$\hat{P}_t^i = AP_{t-1}^i A^T + Q. \quad (2)$$

$$A = \begin{bmatrix} E_{3 \times 3} & O_{3 \times 4} & E_{3 \times 4} \\ O_{4 \times 3} & E_{4 \times 4} & O_{4 \times 4} \\ O_{4 \times 3} & O_{4 \times 4} & E_{4 \times 4} \end{bmatrix}. \quad (3)$$

where \hat{T}_t^i is the predicted state of the trajectory at the current time, T_{t-1}^i means is the state of the trajectory at the previous time, A is the state transition matrix, P_{t-1}^i is the error covariance matrix at the previous time, \hat{P}_t^i is the error covariance matrix at the current time, E and O are the unit and zero matrices respectively, and Q is the covariance matrix of the state function. According to equation (1), the predicted state of the trajectory can be expressed by equations (4), (5) and (6):

$$\hat{x}_t^i = x_{t-1}^i + v_x^i. \quad (4)$$

$$\hat{y}_t^i = y_{t-1}^i + v_y^i. \quad (5)$$

$$\hat{z}_t^i = z_{t-1}^i + v_z^i. \quad (6)$$

In multi-object tracking, all trajectories are generated based on detections in the current frame. Motion of an ego vehicle may lead to errors in motion trajectories between adjacent frames, which requires motion compensation of the ego vehicle. For this purpose, any trajectory $X_{t-1}^C = [x_{t-1}, y_{t-1}, z_{t-1}]^T$ in the camera coordinate system can be first transformed to the IMU coordinate system using equation (7):

$$X_{t-1}^I = T_{C \rightarrow I} X_{t-1}^C. \quad (7)$$

where $T_{C \rightarrow I}$ represents the transformation matrix from the camera coordinate system to the IMU coordinate system.

Based on the pose transformation matrix obtained based on motion of the ego vehicle (by rotating the matrix R_t and translate the matrix T_t), the predicted trajectory state at the

previous time step ($t-1$) can be compensated as expressed in Equation (8), and then transformed from the IMU coordinate system to the camera coordinate system as expressed in Equation (9):

$$X_t^I = R_t X_{t-1}^I + T_t. \quad (8)$$

$$X_t^C = T_{I \rightarrow C} X_t^I. \quad (9)$$

where R_t and T_t respectively represent the rotation matrix and the translation matrix in the pose transformation; $T_{I \rightarrow C}$ represents the transformation matrix from the IMU coordinate system to the camera coordinate system.

C. Trajectory Confidence Fusion Mechanism

Generally speaking, trajectories are generated in the order of the first frame detection, and detectors output detections in a descending order of confidence. This means trajectories are generated in order of confidence at the very beginning, but the order will be disturbed gradually with subsequent continuing matching between trajectories and detections. In [3], it is held that in the data association stage, in terms of detection confidence, trajectories should be associated first with detections of high confidence and then with detections of low confidence. In this paper, the concept of trajectory regression confidence is proposed with reference to the detection confidence-guided data association in the literature, and the confidence of historical trajectories is retained, where upon a NMS processing strategy is further proposed based on the confidence of historical trajectories and effectiveness of the strategy is demonstrated through a large number of experiments.

During tracking, gradual decrease in the regression confidence of an object indicates that the object is gradually disappearing or being occluded. In this case, the object may be considered as a ‘‘weak object’’. On the contrary, an object of high confidence is most likely to be present and thus considered as a ‘‘strong object’’. For these two types of objects, different strategies should be used. Typically, ‘‘strong objects’’ have relatively high detection confidence in the current frame and are easy to match, so they should be matched first. In contrast, ‘‘weak objects’’ generally have low detection confidence, and are liable to be falsely detected or missed in detection due to difficult matching, so they should be matched last. In Fig. 3, the first column shows the object in the red box being gradually occluded by the white vehicle, resulting in gradual decrease in the regression confidence from 0.92 in the 376th frame to 0.30 in the 379th frame; when it comes to the 380th frame, the object is completely occluded and cannot be detected. The second column shows an object gradually disappearing from the field of view. In the second frame, the detection confidence of the object is 0.90, and in the third and fourth frames, it is above 0.75. However, in the fifth frame, only partial front end of the object is in the field of view, when the detection confidence is 0.43. In the sixth frame, the object almost disappears from the field of view, with a detection confidence of only 0.12.



Fig. 3 Illustration of Object Occlusion and Disappearance.

In relation to "strong objects" and "weak objects", a confidence fusion module is introduced in this paper. First, 3D trajectories are input into the detector for regression to obtain corresponding regression confidence. Then, the confidence obtained is fused with the 3D confidence of the trajectory in the previous n frames according to the following equation:

$$S_{3d} = \frac{1}{n+1} (\sum_{k=i-n}^{i-1} S_{3d}^k + S_{3d}^i). \quad (10)$$

where, S_{3d}^i represents the 3D confidence of the trajectory in the current frame, and S_{3d}^k represents previous confidence of the 3D trajectory.

Furthermore, the 2D trajectory generated by the 3D trajectory being projected onto the image is input into the corresponding 2D detector to derive corresponding regression confidence. The confidence so obtained is then fused with the 2D confidence of the trajectory in the previous n frames according to the following formula:

$$S_{2d} = \frac{1}{n+1} (\sum_{k=i-n}^{i-1} S_{2d}^k + S_{2d}^i). \quad (11)$$

where S_{2d}^i represents the 2D confidence of the trajectory in the current frame, and S_{2d}^k represents the previous 2D confidence of the trajectory.

Finally, the 2D confidence (S_{2d}) and 3D confidence (S_{3d}) fused with historical frame information are further fused according to the following formula to obtain the regression confidence of the trajectory:

$$S_f = \frac{1}{2} (S_{3d} + S_{2d}). \quad (12)$$

A high confidence score indicates a high probability of appearing for the trajectory and corresponding object can be considered a "strong object" which should be matched first or otherwise subject to NMS first. On the contrary, a low confidence score indicates the trajectory is being occluded or gradually disappearing from view, and corresponding object can be considered a "weak object" which should be matched with lower priority. Following this principle, all trajectories are sorted according to their confidence scores, as shown in Fig 4.

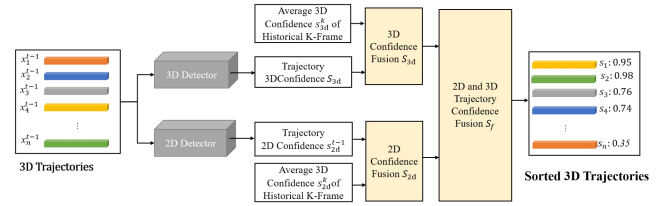


Fig. 4 Schematic Diagram of the Confidence Fusion Module.

D. Post-processing of trajectories

Due to the false negatives produced by detectors, some trajectories may fail to be matched. Combining different modalities of detectors for compensation can solve this problem to some extent. As shown in Fig 5, the vehicle numbered 1 can be detected by both the 2D and 3D detectors in frames 7 and 8; in frame 9, the vehicle is occluded by the black vehicle in front, resulting in production of a false negative by the point cloud-based 3D detector, but at this time it can still be detected by the image-based 2D detector. In this case, the point cloud-based 3D tracker fails to track the trajectory of vehicle 1 in the 9th frame, and if it still fails in the next m frames, the trajectory will change from the confirmed status to the dead status.

To solve the above problem, a post-processing module is added in the present work. If an object is missed by the 3D detector, its trajectory generated in historical frames cannot be matched with detection of the current frame. However, if the regression confidence of the proposed formed by projection of the historical trajectory onto an image in the image-based 2D detector exceeds the set threshold, it is deemed that the trajectory is still in the field of view and the state of the trajectory is confirmed.

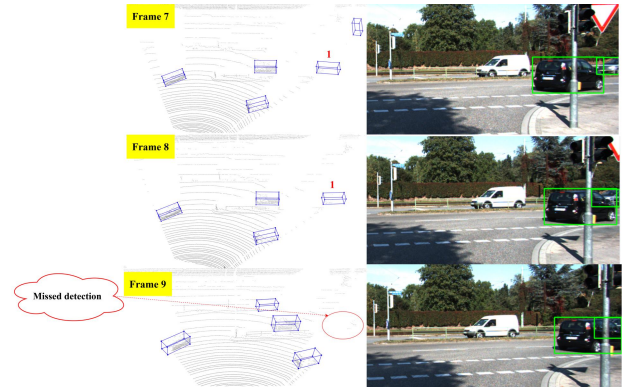


Fig. 5 There is a phenomenon of missed detection in the 3D detector.

IV. EXPERIMENTS

A. Experimental Setup

The proposed fusion framework is implemented using the Python programming language on a desktop computer equipped with an AMD 7950X 4.5 GHz CPU, 64GB RAM, and two RTX 4090 graphics cards.

Datasets: Relevant data from the KITTI dataset [36] and the Waymo dataset [37] are used for experimental validation in this paper. The KITTI dataset is one of the most typical and commonly used datasets in the field of autonomous driving, and it includes 21 training sequences and 29 testing sequences. The training sequences further include a total of 8,008 frames. The testing sequences further include a total of 11,095 frames. The Waymo dataset, as one of the authoritative large-scale datasets currently available, contains 1,150 scenes (1,000 training scenes and 150 testing scenes); each scene lasts for 20 seconds with a frame rate of 10Hz.

Baselines: To prove effectiveness of the proposed method, we have compared the proposed method with the state-of-the-art methods in the current literature, including AB3DMOT [38], JRMOT [39], MOTSFusion [40], GNN3DMOT [18], JMODT [27], Quasi-Dense [41], EagerMOT [17], PC3TMOT [42], LGM [43], DeepFusionMOT [16], OC-SORT [4], PolarMOT [44],

StrongFusionMOT [19], TripletTrack [45], StrongSORT [6], and BcMODT [26].

Evaluation Metrics: In this paper, the proposed method is evaluated by using CLEAR [46] and HOTA [47], among others. CLEAR is commonly used to evaluate the performance of multi-object tracking, and involves evaluation indicators such as Multi-Object Tracking Accuracy (MOTA), Multi-Object Tracking Precision (MOTP), ID Switch (IDS), and others. The CLEAR indicators are subdivided in WAMOY dataset into two levels, i.e. LEVEL_1 (L1) and LEVEL_2 (L2), based on the difficulty in object detection. L1 relates to easy-to-detect objects and L2 relates to difficult-to-detect objects. HOTA is a newly proposed method for multi-object evaluation, and it is currently used as a main evaluation method of tracking performance on the KITTI dataset. HOTA takes into consideration both detection quality and association quality, and involves several indicators, such as detection accuracy (DetA) for evaluating detection performance and association accuracy (AssA) for evaluating association performance.

B. Tracking Performance Evaluation

1) Quantitative Results Analysis: First, the proposed method is validated using the KITTI dataset, and the results are shown in Table I. Data in the table obtained on March 29, 2023, are available at http://www.cvlibs.net/datasets/kitti/old/eval_tracking.php

TABLE I. COMPARISON WITH EXISTING 3D MOT METHODS BY USING THE TEST SET OF THE KITTI CAR TRACKING BENCHMARK. THE BEST RESULTS ARE SHOWN IN BOLD. TBD REFERS TO THE TRACKING-BY-DETECTION PARADIGM, JDE REFERS TO JOINT-DETECTION-EMBEDDING PARADIGM, AND TBC REFERS TO THE JOINT DETECTION AND TRACKING PARADIGM.

| Method | Published (Year) | Type | Input | HOTA (%) \uparrow | AssA (%) \uparrow | AssPr (%) \uparrow | MOTA (%) \uparrow | MOTP (%) \uparrow | IDSW \downarrow | FP \downarrow |
|----------------------|-----------------------------|------|-------|---------------------|---------------------|----------------------|---------------------|---------------------|-------------------|-----------------|
| AB3DMOT [38] | IROS (2020) | TBD | 3D | 69.81 | 69.06 | 89.02 | 83.84 | 85.23 | 126 | 979 |
| JRMOT [39] | IROS (2020) | TBD | 2D+3D | 69.61 | 66.89 | 88.95 | 85.10 | 85.28 | 271 | 787 |
| MOTSFusion [40] | RA-L (2020) | TBD | 2D+3D | 68.74 | 66.16 | 85.49 | 84.24 | 85.03 | 415 | 713 |
| GNN3DMOT [18] | CVPR (2020) | TBD | 2D+3D | ---- | ---- | ---- | 82.40 | ---- | 113 | --- |
| JMODT [27] | IROS (2021) | JDE | 2D+3D | 70.73 | 68.76 | 88.02 | 85.35 | 85.37 | 350 | |
| PC3TMOT [42] | TITS (2021) | TBD | 3D | 77.80 | 81.59 | 88.75 | 88.81 | 84.26 | 225 | 814 |
| Quasi-Dense [41] | CVPR (2021) | TBD | 2D | 68.45 | 65.49 | 88.53 | 84.93 | 84.85 | 313 | 549 |
| EagerMOT [17] | ICRA (2021) | TBD | 2D+3D | 74.39 | 74.16 | 91.15 | 87.82 | 85.69 | 239 | 454 |
| LGM [43] | ICCV (2021) | TBD | 2D | 73.14 | 72.31 | 84.74 | 87.60 | 84.12 | 448 | 1568 |
| DeepFusionMOT [16] | RA-L (2022) | TBD | 2D+3D | 75.46 | 80.06 | 89.77 | 84.64 | 85.02 | 84 | 601 |
| OC-SORT [4] | CVPR (2022) | TBD | 2D | 76.54 | 76.39 | 87.17 | 90.28 | 85.53 | 250 | 407 |
| PolarMOT [44] | ECCV (2022) | TBD | 3D | 75.16 | 76.95 | 89.27 | 85.08 | 85.63 | 462 | 2003 |
| TripletTrack [45] | CVPR (2022) | TBD | 3D | 73.58 | 74.66 | 89.55 | 84.32 | 86.06 | 322 | 430 |
| StrongFusionMOT [19] | IEEE Sensors Journal (2022) | TBD | 2D+3D | 75.65 | 79.84 | 89.81 | 85.53 | 85.07 | 58 | 259 |
| StrongSORT [6] | TMM (2023) | TBD | 2D | 77.75 | 82.20 | 86.73 | 90.35 | 85.42 | 440 | 484 |
| BcMODT [26] | Remote Sensing (2023) | JDE | 2D+3D | 71.00 | 69.14 | 88.70 | 85.48 | 85.31 | 381 | 1260 |
| YONTD-MOT (Ours) | ---- | JDT | 2D+3D | 78.08 | 82.86 | 91.74 | 85.09 | 86.98 | 42 | 1188 |

Table I shows the evaluation results of some recent multi-object tracking methods. According to the results, the proposed method in this paper has significant advantages in terms of HOTA, DetA, AssA, MOTP, IDSW, and other indicators. For HOTA, 78.08% is achieved by using the proposed method in this paper, having improved by 2.62%

over that achieved by using our previous DeepFusionMOT [16] and by 2.43% over that achieved by using our previous StrongFusionMOT [19]. For MOTP, an indicator focusing on the positional accuracy of trajectory boxes, the highest score of 86.98 is achieved by using the proposed method in this paper among all methods in the table. For AssA, an indicator focusing on the accuracy of association, 82.86% is achieved

by using the proposed method in this paper, which is a significant improvement in comparison to other latest multi-modal fusion methods such as DeepFusionMOT (80.06%), StrongFusionMOT [19] (79.84%), and EagerMOT [17] (74.16%). In addition, the proposed method in this paper has the least number of ID switches, i.e. only 42 times, which demonstrates its robustness.

To verify applicability of the proposed method in this paper, another large dataset Waymo is used for evaluation. The dataset comprises a total of 3 categories. Experimental results are shown in Table II. Data in the table are sourced from submissions to the Waymo dataset website on March 29, 2023. For more details, please visit <https://Waymo.com/open/challenges/2020/3d-tracking/>.

It can be known from Table II that the proposed method in this paper also performs well on the Waymo dataset, having delivered the best tracking performance among the methods in comparison. Specifically, significant improvement is seen in multiple indicators with the proposed method in this paper when compared with the baseline method `pillars_kf_baseline` [37] on the Waymo website. For example, there is an improvement of 30.15% in terms of MOTA (L1), 29.78% in terms of MOTA (L2), 6.50% in terms of MOTP (L1), and 6.54% in terms of MOTP (L2). Compared with other latest methods, such as Probabilistic 3DMOT[48], the proposed method in this paper has significant improvements in indicators such as MOTA (L1/L2) and MOTP (L1/L2).

TABLE II. COMPARISON WITH EXISTING 3D MOT METHODS BY USING THE TEST SET OF THE WAYMO TRACKING BENCHMARK. THE BEST RESULTS ARE SHOWN IN BOLD.

| Method | Published (Year) | Input | MOTA/L1 (%) \uparrow | MOTP/L1 (%) \uparrow | FP/L1 (%) \downarrow | MOTA/L2 (%) \uparrow | MOTP/L2 (%) \uparrow | FP/L2 (%) \downarrow |
|---------------------------------------|------------------|-------|------------------------|------------------------|------------------------|------------------------|------------------------|------------------------|
| <code>pillars_kf_baseline</code> [37] | CVPR (2020) | 3D | 27.13 | 17.53 | 9.78 | 25.92 | 17.53 | 9.32 |
| PV-RCNN-KF [49] | CVPR (2020) | 3D | 57.14 | 24.95 | 8.72 | 55.53 | 24.97 | 8.66 |
| 2-stage data assoc [50] | Sensors (2021) | 3D | 37.91 | 26.26 | 9.18 | 36.53 | 26.26 | 8.85 |
| Probabilistic 3DMOT [48] | ICRA (2021) | 3D | 49.16 | 24.80 | 9.13 | 47.65 | 24.82 | 8.99 |
| YONTD-MOT (Ours) | --- | 2D+3D | 57.28 | 24.03 | 8.24 | 55.70 | 24.07 | 8.44 |

2) Qualitative Results Analysis:

Fig. 6 and Fig. 7 show two visual examples of comparison with the latest trackers. Fig. 6 shows 0001 sequence in the KITTI training set, where the first and second rows represent the 3D detection results of a certain frame. The first column in the third row is the ground truth trajectory, the second column is the visualization result of the proposed method, the third column is the result of the PC3TMOT method, the fourth column is the tracking result of the DeepFusionMOT method, and the fifth column is the tracking result of the AB3DMOT method. From the figure, it can be seen that ID switches have occurred to trajectories with ID 90 and ID 91 in the

PC3TMOT method, and the trajectory with ID 81 has the ID switch to ID 82 in the subsequent frames. In the DeepFusionMOT method, the trajectory with ID 83 has the ID switch to ID 86. ID switch is also observed in AB3DMOT. In contrast, the proposed method in this paper exhibits strong robustness in handling complex scenarios such as intersections with object occlusion and disappearance, without any ID switch. Fig. 7 shows 0010 sequence in the KITTI test set, corresponding to a crossroad scene with object occlusion. In this circumstance, the proposed method also shows more robust performance compared to AB3DMOT and PC3TMOT.

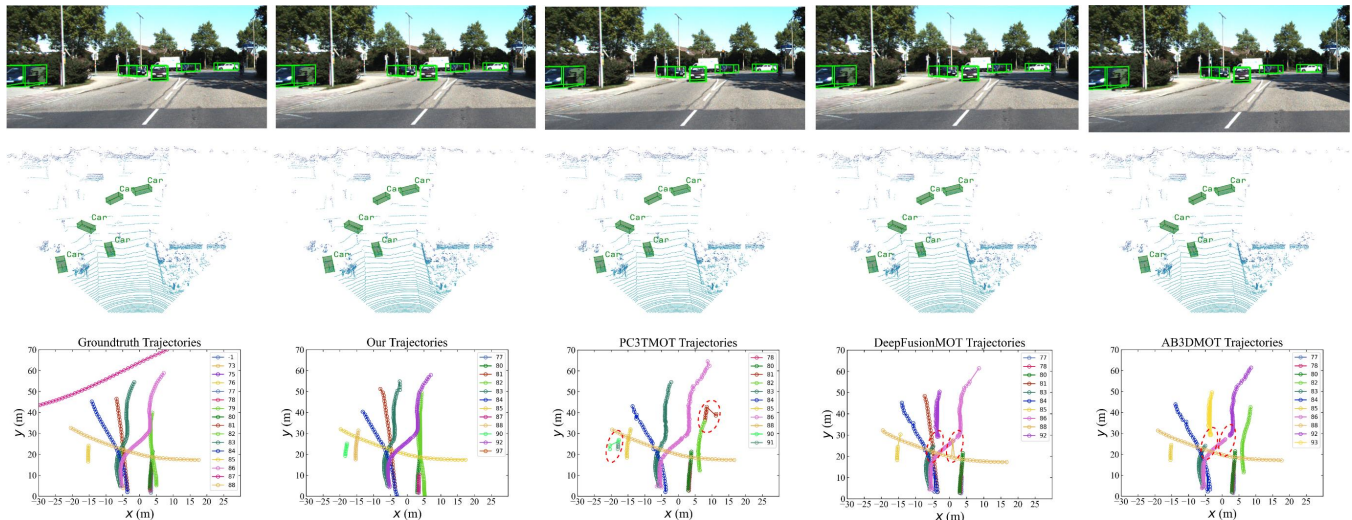


Fig.6 A comparison of bird's eye view trajectories between our method and other methods including PC3TMOT, DeepFusionMOT, AB3DMOT using a KITTI data sequence. Trajectories with the same ID are shown in the same color. The red circle in the figure indicates that there is an ID switch in the trajectory.

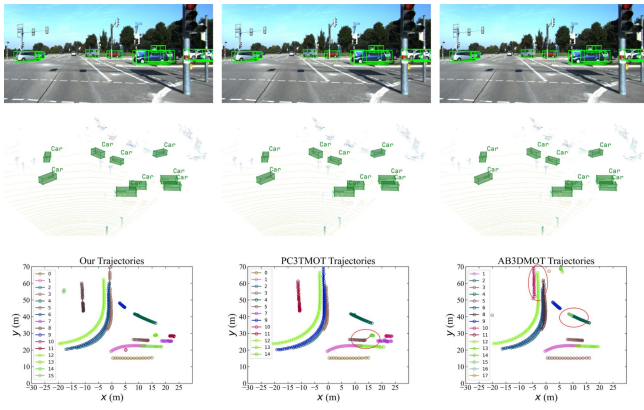


Fig. 7 Another example of visual comparison between our method and other methods. The red circle in the figure indicates that there is an ID switch in the trajectory.

C. Ablation Study

In order to explore impact of different modules on the overall tracking performance, ablation experiments are conducted with validation sets in KITTI and Waymo datasets. The KITTI validation set is randomly divided into 11 sequences, including 0000, 0002, 0005, 0006, 0008, 0009, 0012, 0014, 0016, 0018, 0019. Evaluation is performed in terms of CLEAR and HOTA.

① Impact of 2D Detector

The multi-object tracking framework proposed in this paper can achieve high-precision tracking with a 2D detector. Removal of the 2D detector may reduce the framework to point cloud-based end-to-end multi-object tracking, and thereby affect the tracking performance to some extent. As shown in Table III, removal of the 2D detector leads to significant reduction in comprehensive indicators such as HOTA, AssA, and MOTA, mainly due to the significant increase in missed objects. At the same time, increase in missed objects results in decrease in the total number of tracking trajectories, and further causes decrease in FP and IDSW. In summary, the 2D detector can provide more accurate object detection information for the method proposed in this paper, thereby improving the tracking accuracy and robustness of the system.

TABLE III. ABLATION STUDY - IMPACT OF 2D DETECTORS ON TRACKING PERFORMANCE

| Detector | HOTA (%) \uparrow | AssA (%) \uparrow | MOTA (%) \uparrow | FN \downarrow |
|----------|---------------------|---------------------|---------------------|-----------------|
| 3D + 2D | 76.37 | 80.63 | 80.41 | 1424 |
| Only 3D | 73.60 | 79.60 | 74.63 | 2268 |

② Impact of Object Detectors

In order to study the impact of different detectors on the overall tracking performance, three 3D detectors (i.e. CasA [35], PointRCNN [20], and Voxel R-CNN [21]) and two 2D detectors (i.e. Faster R-CNN [25] and Mask R-CNN [51]) are selected in the present work. Experimental results are shown in Table IV. According to the results, when Voxel R-CNN and Faster R-CNN are used, the highest HOTA and MOTA, and the least FN are achieved. In contrast, combined use of PointRCNN and Mask R-CNN delivers the worst results.

TABLE IV. ABLATION STUDY - IMPACT OF DIFFERENT OBJECT DETECTORS

| 3D Detector | 2D Detector | HOTA (%) \uparrow | MOTA (%) \uparrow | FN \downarrow |
|------------------|-------------------|---------------------|---------------------|-----------------|
| CasA [35] | Faster R-CNN [25] | 76.37 | 80.41 | 1424 |
| | Mask R-CNN [51] | 75.30 | 77.81 | 1667 |
| PointRCNN [20] | Faster R-CNN [25] | 53.11 | 43.96 | 4721 |
| | Mask R-CNN [51] | 55.02 | 46.59 | 4495 |
| Voxel R-CNN [21] | Faster R-CNN [25] | 77.52 | 82.11 | 610 |
| | Mask R-CNN [51] | 76.50 | 80.36 | 786 |

③ Confidence Fusion Module

In order to investigate the impact of the trajectory and detection NMS order on tracking performance, or the role of the proposed Confidence Fusion Module in this paper, three sets of experiments are conducted using the KITTI and Waymo validation sets: orderless NMS, NMS in descending order of confidence, and NMS in ascending order of confidence. Experimental results are shown in Table V and Table VI. According to Table V, when the trajectory regression confidence is sorted in descending order, best results of important indicators such as HOTA, Ass, and MOTA are achieved. Similarly, according to Table VI where experimental results of the three categories (VEHICLE, PEDESTRIAN, CYCLIST) are shown, when the trajectory confidence is sorted in descending order, best results of MOTP and MISS, as well as outstanding results of MOTA, MISMATCH and FP, are achieved. All experimental results above suggest that the Confidence Fusion Module proposed in this paper can improve tracking performance.

TABLE V. ABLATION STUDY - IMPACT OF DIFFERENT OBJECT DETECTORS

| Confidence order | HOTA (%) \uparrow | AssA (%) \uparrow | MOTA (%) \uparrow | FN |
|------------------|---------------------|---------------------|---------------------|-------------|
| Unordered | 74.90 | 78.40 | 79.49 | 1519 |
| Ascending | 75.73 | 79.98 | 79.58 | 1534 |
| Descending | 76.37 | 80.63 | 80.41 | 1424 |

TABLE VI. ABLATION STUDY - IMPACT OF DIFFERENT OBJECT DETECTORS

| Category | Confidence order | MOTA (%) \uparrow | MISS (%) \downarrow | MISMATCH (%) \downarrow |
|------------|------------------|---------------------|-----------------------|---------------------------|
| VEHICLE | Unordered | 52.70 | 15.82 | 0.32 |
| | Ascending | 45.30 | 15.82 | 7.46 |
| | Descending | 53.02 | 15.83 | 0.40 |
| PEDESTRIAN | Unordered | 47.85 | 31.39 | 1.68 |
| | Ascending | 40.59 | 31.38 | 9.79 |
| CYCLIST | Descending | 47.45 | 31.40 | 1.00 |
| | Unordered | 40.13 | 22.35 | 0.50 |
| | Ascending | 34.51 | 22.35 | 5.45 |
| | Descending | 40.45 | 22.38 | 0.35 |

④ Retained frames of a trajectory

In the trajectory management strategy of the present work, when a confirmed trajectory does not match detection in a certain frame, the trajectory status will change from "confirmed" to "reappearing", and the *max_age* frame of the trajectory is retained. Once the trajectory matches again with detection in the *max_age* frame, the status will change back to "confirmed". Experimental results show that selection of *max_age* has a significant impact on the tracking performance. In the present work, the entire training set of the KITTI dataset is used in experiments. The experimental

results are shown in Fig. 8. According to the figure, as max_age increases, both FP and TP take a rise trend, and MOTA also increases accordingly. However, after max_age reaches 92, FP continues to increase while TP remains almost unchanged. This indicates that when a trajectory disappears briefly, it should not be deleted immediately, nor retained for too long; the number of frames that trajectory is retained needs to be appropriately selected. Therefore, in the trajectory management strategy, the selection of max_age needs to be adjusted according to specific application scenarios and experimental results to improve tracking performance.

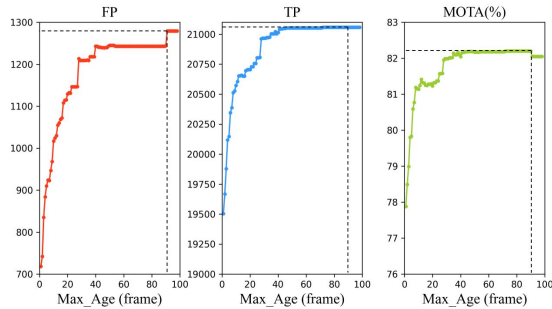


Fig. 8 The impact of the number of frames with preserved trajectories on tracking performance.

⑤ Number of trajectory frames to be fused

In the confidence fusion module, it is necessary to fuse confidence of multiple historical frames, so as to better determine the status of a trajectory ("strong" or "weak") in the current frame. The number of historical frames, chm , has great impact on the tracking performance. As shown in Fig 9, as chm increases, FP decreases first and then increases, while TP and MOTA increase first and then decrease. The optimal result is achieved when $chm = 10$. These results suggest that the current status of a trajectory can be best reflected not by fusing too many historical frames of confidence, and the maximum improvement in tracking performance is achieved by fusing the most recent 10 frames of data (under the experimental conditions in this paper). Therefore, in practical applications, an appropriate chm should be selected based on specific circumstances to improve the performance of a tracker.

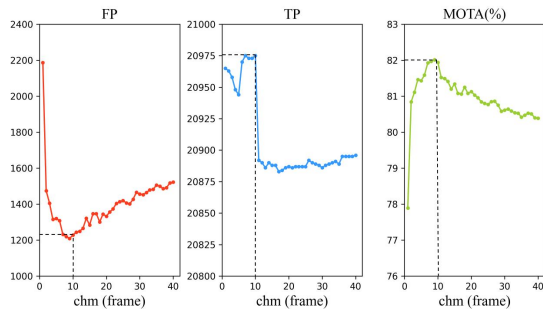


Fig. 9 Impact of Fusing Historical Trajectory Frames on Tracking Performance

V. CONCLUSION AND FUTURE WORK

In this paper, a new multi-object tracking framework is proposed based on multimodal fusion. The framework can achieve good tracking performance without the need for

complex data association processes and outperform many multimodal tracking methods that use various features for association. For the purpose of the present work, use of trajectory regression confidence to characterize the trajectory state (strong object or weak object) is proposed for the first time, and trajectories are sorted for ordered tracking. According to evaluation of the proposed method with KITTI and Waymo datasets, state-of-the-art performance is achieved in the KITTI dataset in comparison to multimodal fusion-based methods on the leaderboard, and good tracking performance is achieved in the Waymo dataset.

REFERENCES

- [1] A. Bewley, Z. Ge, L. Ott, F. Ramos, and B. Upcroft, "Simple online and realtime tracking," in *2016 IEEE international conference on image processing (ICIP)*, 2016, pp. 3464-3468: IEEE.
- [2] N. Wojke, A. Bewley, and D. Paulus, "Simple online and realtime tracking with a deep association metric," in *2017 IEEE international conference on image processing (ICIP)*, 2017, pp. 3645-3649: IEEE.
- [3] Y. Zhang *et al.*, "Bytetrack: Multi-object tracking by associating every detection box," in *Computer Vision—ECCV 2022: 17th European Conference, Tel Aviv, Israel, October 23–27, 2022, Proceedings, Part XXII*, 2022, pp. 1-21: Springer.
- [4] J. Cao, X. Weng, R. Khirodkar, J. Pang, and K. Kitani, "Observation-centric sort: Rethinking sort for robust multi-object tracking," *arXiv preprint arXiv:2203.14360*, 2022.
- [5] L. Wang *et al.*, "CAMO-MOT: Combined Appearance-Motion Optimization for 3D Multi-Object Tracking with Camera-LiDAR Fusion," *arXiv preprint arXiv:2209.02540*, 2022.
- [6] Y. Du *et al.*, "StrongSORT: Make DeepSORT Great Again," in *IEEE Transactions on Multimedia*, doi: 10.1109/TMM.2023.3240881.
- [7] J. He, C. Fu, and X. Wang, "3D Multi-Object Tracking Based on Uncertainty-Guided Data Association," *arXiv preprint arXiv:2303.01786*, 2023.
- [8] Z. Wang, L. Zheng, Y. Liu, Y. Li, and S. Wang, "Towards real-time multi-object tracking," in *Computer Vision—ECCV 2020: 16th European Conference, Glasgow, UK, August 23–28, 2020, Proceedings, Part XI 16*, 2020, pp. 107-122: Springer.
- [9] Y. Zhang, C. Wang, X. Wang, W. Zeng, and W. Liu, "FairMOT: On the Fairness of Detection and Re-identification in Multiple Object Tracking," *International Journal of Computer Vision*, pp. 3069–3087, Sep. 2021.
- [10] P. Sun *et al.*, "Transtrack: Multiple object tracking with transformer," *arXiv preprint arXiv:2012.15460*, 2020.
- [11] T. Meinhardt, A. Kirillov, L. Leal-Taixe, and C. Feichtenhofer, "Trackformer: Multi-object tracking with transformers," in *Proceedings of the IEEE/CVF conference on computer vision and pattern recognition*, 2022, pp. 8844-8854.
- [12] P. Chu, J. Wang, Q. You, H. Ling, and Z. Liu, "Transmot: Spatial-temporal graph transformer for multiple object tracking," in *Proceedings of the IEEE/CVF Winter Conference on Applications of Computer Vision*, 2023, pp. 4870-4880.
- [13] P. Bergmann, T. Meinhardt, and L. Leal-Taixe, "Tracking without bells and whistles," in *Proceedings of the IEEE/CVF International Conference on Computer Vision*, 2019, pp. 941-951.
- [14] J. Zhang *et al.*, "Multiple object tracking by flowing and fusing," *arXiv preprint arXiv:2001.11180*, 2020.
- [15] X. Zhou, V. Koltun, and P. Krähenbühl, "Tracking objects as points," in *Computer Vision—ECCV 2020: 16th European Conference, Glasgow, UK, August 23–28, 2020, Proceedings, Part IV*, 2020, pp. 474-490: Springer.
- [16] X. Wang, C. Fu, Z. Li, Y. Lai, and J. He, "DeepFusionMOT: A 3D Multi-Object Tracking Framework Based on Camera-LiDAR Fusion With Deep Association," *IEEE Robotics and Automation Letters*, vol. 7, no. 3, pp. 8260-8267, 2022.
- [17] A. Kim, A. Osep, and L. Leal-Taixe, "EagerMOT: 3D Multi-Object Tracking via Sensor Fusion," in *2021 IEEE International Conference on Robotics and Automation (ICRA)*, Xi'an, China, Oct. 2021. doi: 10.1109/icra48506.2021.9562072.

- [18] X. Weng, Y. Wang, Y. Man, and K. M. Kitani, "Gnn3dmot: Graph neural network for 3d multi-object tracking with 2d-3d multi-feature learning," in *Proceedings of the IEEE/CVF Conference on Computer Vision and Pattern Recognition*, 2020, pp. 6499-6508.
- [19] X. Wang, C. Fu, J. He, S. Wang and J. Wang, "StrongFusionMOT: A Multi-Object Tracking Method Based on LiDAR-Camera Fusion," in *IEEE Sensors Journal*, doi: 10.1109/JSEN.2022.3226490.
- [20] S. Shi, X. Wang, and H. Li, "Pointcnn: 3d object proposal generation and detection from point cloud," in *Proceedings of the IEEE/CVF conference on computer vision and pattern recognition*, 2019, pp. 770-779.
- [21] J. Deng, S. Shi, P. Li, W. Zhou, Y. Zhang, and H. Li, "Voxel r-cnn: Towards high performance voxel-based 3d object detection," in *Proceedings of the AAAI Conference on Artificial Intelligence*, 2021, vol. 35, no. 2, pp. 1201-1209.
- [22] W. Shi and R. Rajkumar, "Point-gnn: Graph neural network for 3d object detection in a point cloud," in *Proceedings of the IEEE/CVF conference on computer vision and pattern recognition*, 2020, pp. 1711-1719.
- [23] J. Ren *et al.*, "Accurate single stage detector using recurrent rolling convolution," in *Proceedings of the IEEE conference on computer vision and pattern recognition*, 2017, pp. 5420-5428.
- [24] Z. Ge, S. Liu, F. Wang, Z. Li, and J. Sun, "Yolox: Exceeding yolo series in 2021," *arXiv preprint arXiv:2107.08430*, 2021.
- [25] S. Ren, K. He, R. Girshick, and J. Sun, "Faster r-cnn: Towards real-time object detection with region proposal networks," *Advances in neural information processing systems*, vol. 28, 2015.
- [26] K. Zhang, Y. Liu, F. Mei, J. Jin, and Y. Wang, "Boost Correlation Features with 3D-MIoU-Based Camera-LiDAR Fusion for MODT in Autonomous Driving," *Remote Sensing*, vol. 15, no. 4, p. 874, 2023.
- [27] K. Huang and Q. Hao, "Joint Multi-Object Detection and Tracking with Camera-LiDAR Fusion for Autonomous Driving," 2021 *IEEE/RSJ International Conference on Intelligent Robots and Systems (IROS)*, Prague, Czech Republic, 2021, pp. 6983-6989.
- [28] E. Bochinski, V. Eiselein, and T. Sikora, "High-speed tracking-by-detection without using image information," in *2017 14th IEEE International Conference on Advanced Video and Signal Based Surveillance (AVSS)*, 2017, pp. 1-6: IEEE.
- [29] A. Vaswani *et al.*, "Attention is all you need," *Advances in neural information processing systems*, vol. 30, 2017.
- [30] N. Carion, F. Massa, G. Synnaeve, N. Usunier, A. Kirillov, and S. Zagoruyko, "End-to-end object detection with transformers," in *Computer Vision—ECCV 2020: 16th European Conference, Glasgow, UK, August 23–28, 2020, Proceedings, Part I 16*, 2020, pp. 213-229: Springer.
- [31] X. Zhu, W. Su, L. Lu, B. Li, X. Wang, and J. Dai, "Deformable detr: Deformable transformers for end-to-end object detection," *arXiv preprint arXiv:2010.04159*, 2020.
- [32] J. Beal, E. Kim, E. Tzeng, D. H. Park, A. Zhai, and D. Kislyuk, "Toward transformer-based object detection," *arXiv preprint arXiv:2012.09958*, 2020.
- [33] A. Milan, L. Leal-Taixé, I. Reid, S. Roth, and K. Schindler, "MOT16: A benchmark for multi-object tracking," *arXiv preprint arXiv:1603.00831*, 2016.
- [34] P. Dendorfer *et al.*, "Mot20: A benchmark for multi object tracking in crowded scenes," *arXiv preprint arXiv:2003.09003*, 2020.
- [35] H. Wu, J. Deng, C. Wen, X. Li, C. Wang, and J. Li, "CasA: A cascade attention network for 3-D object detection from LiDAR point clouds," *IEEE Transactions on Geoscience and Remote Sensing*, vol. 60, pp. 1-11, 2022.
- [36] A. Geiger, P. Lenz, and R. Urtasun, "Are we ready for autonomous driving? the kitti vision benchmark suite," in *2012 IEEE conference on computer vision and pattern recognition*, 2012, pp. 3354-3361: IEEE.
- [37] P. Sun *et al.*, "Scalability in perception for autonomous driving: Waymo open dataset," in *Proceedings of the IEEE/CVF conference on computer vision and pattern recognition*, 2020, pp. 2446-2454.
- [38] X. Weng, J. Wang, D. Held, and K. Kitani, "3d multi-object tracking: A baseline and new evaluation metrics," in *2020 IEEE/RSJ International Conference on Intelligent Robots and Systems (IROS)*, 2020, pp. 10359-10366: IEEE.
- [39] A. Shenoi *et al.*, "Jrmt: A real-time 3d multi-object tracker and a new large-scale dataset," in *2020 IEEE/RSJ International Conference on Intelligent Robots and Systems (IROS)*, 2020, pp. 10335-10342: IEEE.
- [40] J. Luiten, T. Fischer, and B. Leibe, "Track to Reconstruct and Reconstruct to Track," *IEEE Robotics and Automation Letters*, vol. 5, no. 2, pp. 1803-1810, Jan. 2020, doi: 10.1109/lra.2020.2969183.
- [41] J. Pang *et al.*, "Quasi-dense similarity learning for multiple object tracking," in *Proceedings of the IEEE/CVF Conference on Computer Vision and Pattern Recognition*, 2021, pp. 164-173.
- [42] H. Wu, W. Han, C. Wen, X. Li, and C. Wang, "3D Multi-Object Tracking in Point Clouds Based on Prediction Confidence-Guided Data Association," *IEEE Transactions on Intelligent Transportation Systems*, pp. 5668-5677, Feb. 2021, doi: 10.1109/its.2021.3055616.
- [43] G. Wang, R. Gu, Z. Liu, W. Hu, M. Song, and J.-N. Hwang, "Track Without Appearance: Learn Box and Tracklet Embedding With Local and Global Motion Patterns for Vehicle Tracking," in *Proceedings of the IEEE/CVF International Conference on Computer Vision*, 2021, pp. 9876-9886.
- [44] A. Kim, G. Brasó, A. Ošep, and L. Leal-Taixé, "PolarMOT: How far can geometric relations take us in 3D multi-object tracking?," in *Computer Vision—ECCV 2022: 17th European Conference, Tel Aviv, Israel, October 23–27, 2022, Proceedings, Part XXII*, 2022, pp. 41-58: Springer.
- [45] N. Marinello, M. Proesmans, and L. Van Gool, "TripletTrack: 3D Object Tracking using Triplet Embeddings and LSTM," in *Proceedings of the IEEE/CVF Conference on Computer Vision and Pattern Recognition*, 2022, pp. 4500-4510.
- [46] K. Bernardin and R. Stiefelhagen, "Evaluating Multiple Object Tracking Performance: The CLEAR MOT Metrics," *EURASIP Journal on Image and Video Processing*, pp. 1-10, Jun. 2008, doi: 10.1155/2008/246309.
- [47] J. Luiten *et al.*, "HOTA: A Higher Order Metric for Evaluating Multi-object Tracking," *International Journal of Computer Vision*, pp. 548-578, Oct. 2020, doi: 10.1007/s11263-020-01375-2.
- [48] H. -K. Chiu, J. Li, R. Ambruş and J. Bohg, "Probabilistic 3D Multi-Modal, Multi-Object Tracking for Autonomous Driving," 2021 *IEEE International Conference on Robotics and Automation (ICRA)*, Xi'an, China, 2021, pp. 14227-14233.
- [49] S. Shi *et al.*, "Pv-rnn: Point-voxel feature set abstraction for 3d object detection," in *Proceedings of the IEEE/CVF Conference on Computer Vision and Pattern Recognition*, 2020, pp. 10529-10538.
- [50] M.-Q. Dao and V. Frémont, "A two-stage data association approach for 3D Multi-object Tracking," *Sensors*, vol. 21, no. 9, p. 2894, 2021.
- [51] K. He, G. Gkioxari, P. Dollár, and R. Girshick, "Mask r-cnn," in *Proceedings of the IEEE international conference on computer vision*, 2017, pp. 2961-2969.